ARTICLE

BIOTECHNOLOGY and BIOENGINEERING

Bioreducible Poly(Amido Amine)s With Different Branching Degrees as Gene Delivery Vectors

Bo Zhang,[1,2,†] Xinpeng Ma,[2] William Murdoch,[3] Maciej Radosz,[2] Youqing Shen[1,2]

[1]Center for Bionanoengineering and the State Key Laboratory for Chemical Engineering, Department of Chemical and Biological Engineering, Zhejiang University, Hangzhou, China 310027; telephone: 86-571-87953993; fax: 86-571-87953993; e-mail: shenyq@zju.edu.cn

[2]Department of Chemical and Petroleum Engineering, University of Wyoming, Laramie, Wyoming 82071

[3]Department of Animal Science, University of Wyoming, Laramie, Wyoming 82071

ABSTRACT: Based on the knowledge that cationic polymers with different topographical structures behave differently in gene transfection process, herein, we synthesized three biodegradable poly(amido amine)s (PAAs) with the same repeating units and molecular weights except for degree of branching: linear PAA (LPAA), low-branched PAA (LBPAA), and high-branched PAA (HBPAA). We found that LBPAA could more effectively compact pDNA into positively charged nanoparticles than both HBPAA and LPAA. LBPAA polyplexes had the highest transfection efficiency among the three PAA polyplexes, and the difference in transfection efficiency is mainly attributed to the endocytosis rate. The cytotoxicity of PAAs was negligible at the transfection doses, probably due to the degradable disulfide bonds. Therefore, we could use branching as a parameter to simply tune a polymer's cellular uptake behavior and transfection efficiency.

Biotechnol. Bioeng. 2013;110: 990–998.

KEYWORDS: gene delivery; nonviral; poly(amido amine); degree of branching; disulfide bond

Correspondence to: Y. Shen
[†]Visiting student to ZJU.
Contract grant sponsor: National Nature Science Fund for Distinguished Young Scholars
Contract grant number: 50888001
Contract grant sponsor: National Natural Science Foundation of China
Contract grant number: 20974096
Contract grant sponsor: U.S. National Science Foundation
Contract grant number: CBET 0753109; DMR-0705298
Contract grant sponsor: Department of Defense
Contract grant number: BC083821
Received 22 August 2012; Revision received 15 October 2012; Accepted 18 October 2012
Accepted manuscript online 23 October 2012;
Article first published online 23 November 2012 in Wiley Online Library (http://onlinelibrary.wiley.com/doi/10.1002/bit.24772/abstract)
DOI 10.1002/bit.24772

Introduction

Gene therapy is a promising approach to treat genetic disorders (Zeng et al., 2010). While the clinical applications of viral vectors are largely limited due to their safety issues (Cho and Kwon, 2012; Thomas et al., 2003), nonviral carriers exhibit unique advantages such as low toxicity, biodegradability, tissue/tumor targeting, and applicable scale-up to production (Kibria et al., 2011; Tzeng et al., 2011). In recent years, a variety of cationic polymers, such as polyethyleneimine (PEI) (Zeng et al., 2010), poly(L-lysine) (von Erlach et al., 2011), and polyamidoamine dendrimers (Han et al., 2011), have been studied intensively as gene carriers (Lin and Engbersen, 2008). However, polymeric gene delivery systems have relatively low transfection efficiencies compared to their viral counterparts. Therefore, great effort has been dedicated to their improvement. One of the most important directions is the rational design of new polymer structures and understanding how the polymer structural factors influence gene transfection efficacy.

Recently, a new class of biodegradable poly(amido amine)s (PAA) containing disulfide linkages in the backbone were developed for gene delivery (Brumbach et al., 2010; Liu et al., 2010; Meng et al., 2009; Ou et al., 2009; Piest and Engbersen, 2010; Vader et al., 2011; Yang et al., 2011). Such polymers formed stable polyplexes with DNA, but once inside the cells these disulfide bonds were cleaved by the intracellular glutathione, whose concentration was 100–1,000 times higher than that in extracellular fluids (Wu et al., 2004), leading to polyplex disassociation and effective DNA release. Another advantage of these polymers is low toxicity due to their degradability (Ou et al., 2008).

Compared to their linear counterparts (Parhamifar et al., 2010), branched cationic polymers have different types of amines, and thus different basicity and degree of protonation, which might influence their interactions with cell membranes and thereby cellular uptake, endosomal escape

and transfection processes (Dai et al., 2011; Jiang et al., 2011). For instance, partially degraded polyamidoamine dendrimers achieved higher transfection efficiency than did intact dendrimers due to the increased flexibility and enhanced buffering capacity in endosomes (Tang et al., 1996). Poly(amido amine)s with the same repeating units but different degrees of branching (DB) might impart polymers with different buffering capacity, zeta potential and transfection efficiency (Wang et al., 2010). Therefore, branching provides another parameter to tune the polymer properties needed for efficient gene delivery (Zhou et al., 2010; Zhu et al., 2011).

In this work, we studied how DB affected the endocytosis and gene transfection. We found that branching strongly affected the PAA's pDNA compaction, pDNA binding, cellular uptake, and transfection efficiency.

Materials and Methods

Materials

Cystaminedihydrochloride (≥98.0%), sodium hydroxide (≥98.0%), acryloyl chloride (97%), and 1-(2-aminoethyl)-piperazine (99%), chlorpromazine, Filipin III and wortmannin were purchased from Sigma–Aldrich (Milwaukee, WI). Anhydrous dichloromethane (99.96%) and acetone (99.0%) were purchased from Fisher Scientific (Pittsburgh, PA). Linear polyethyleneimine (LPEI 25 KDa), hydrochloric acid (37%), and sodium hydroxide (99.8%) were from Fisher Scientific. Anhydrous dimethyl sulfoxide (DMSO, 99.9%) and *N*,*N*-dimethylformamide (DMF, 99.9%) were from EMD Chemicals (Gibbstown, NJ). pGL4 luciferase reporter vectors, *Escherichia coli*. competent cells and luciferase assay system were purchased from Promega (Madison, WI). QIAGEN plasmid Midi Kit was purchased from Qiagen (Valencia, CA). *Label*IT® Nucleic Acid Labeling Kit, Cy™ 5 was purchased from Mirus Bio (Madison, WI).

Synthesis of *N,N′*-Cystaminebisacrylamide (CBA) and PAAs With Different DBs

CBA was synthesized according to the literature (Emilitri et al., 2005; Sun et al., 2008). ^{1}H NMR ($CDCl_3$, 400 Hz): δ (ppm): 6.66 (b, 2H), 6.35 (d, $J = 17.2$ Hz, 2H), 6.31 (m, 2H), 5.69 (d, $J = 10$ Hz, 2H), 3.69 (m, 4H), 2.90 (t, $J = 6.8$ Hz, 4H).

Linear PAA (LPAA) was synthesized by Michael addition between CBA and 1-(2-aminoethyl)piperazine (AEPZ) according to the literature (Wang et al., 2010). Briefly, CBA and AEPZ were dissolved in DMF under the protection of nitrogen. The solution was stirred at 60°C for 3 days. The product was collected by centrifugation as a yellow solid. ^{1}H NMR ($CDCl_3$, 400 Hz): δ (ppm): 8.42 (b), 3.39 (b), 2.89 (b), 2.73 (b), 2.57 (b), 2.43 (b), 2.35 (b).

Low-branched PAA (LBPAA) was synthesized by the same procedure as for LPAA except in a mixed solvent DMF/H_2O (volume ratio of 4/1). ^{1}H NMR ($CDCl_3$, 400 Hz): δ (ppm): 8.13 (b), 3.32 (t, $J = 6$ Hz), 2.77 (m), 2.48 (b), 2.36 (b).

High-branched PAA (HBPAA) was synthesized by the same procedure as for LPAA except in a mixed solvent DMF/H_2O (volume ratio of 1/2). ^{1}H NMR ($CDCl_3$, 400 Hz): δ (ppm): 8.33 (b), 3.32 (b), 2.74 (b), 2.65 (b), 2.57 (b), 2.47 (b), 2.36 (b), 2.23 (b).

Preparation of Plasmid DNA

The plasmids were propagated in Top 10 *E. coli*. competent cells in Luria–Bertanic (LB) agar broth supplemented with 50 μg/mL kanamycin (Sigma, Milwaukee, WI) at 37°C. The mixture was gently shaken overnight at 200 rpm. The pDNA was purified using QIAGEN plasmid Midi Kit according to the manufacturer's instruction. The pDNA concentration was determined by measuring its UV-absorbance at 260 nm. The pDNA purity was determined by measuring its optical density (OD) with Nanodrop ND-1000 (Thermo Scientific, Waltham, MA), and the pDNA with an OD 260/280 nm ratio between 1.8 and 2.0 was used. The pGL4 plasmids were verified by 0.9% agarose gel electrophoresis to confirm that there was no gene rearrangement during cloning and propagation. pDNA aliquots were stored at −20°C prior to use.

Gel Electrophoresis

PAA/pDNA complexes were formed by adding 10 μL of a pDNA solution (pGL4-luc, 40 μg/mL) to the same volume of polymer solutions at various concentrations to yield the desired PAA/pDNA weight ratios followed by 15 s of vortexing. In the DTT degradation study, 2 μL of DTT solution was added to the above mixture to give the final concentration of 10 mM DTT, followed by 1 h incubation at 37°C. Polyplexes with or without DTT were electrophoresed on a 0.9% agarose gel at 100 V for 40 min. pDNA bands were visualized by staining with ethidium bromide (EB) and observed under UV light.

Size and Zeta Potential Measurements

The sizes of polyplexes were determined using a Nano-ZS zetasizer (Malvern Instrument, Great Malvern, UK) with a laser light wavelength of 632.8 nm and scattering angle at 173°. The polyplexes were prepared as described above, except that the total volume of polyplex solutions was increased to 1 mL. Each measurement was performed at 25°C for 30 runs in triplicate, and the results were processed with DTS software version 3.32.

The zeta potentials were determined using phase-analysis light-scattering technology with the zetasizer. The

measurements were performed in disposable zeta capillary cells at 25°C for 30 runs in triplicate, and the results were processed with DTS software version 3.32.

Ethidium Bromide Replacement Assay

pDNA 50 μL (40 μg/mL) and an equal volume of PAA at various concentrations to yield different polymer/DNA ratios (e.g., 1 mg/mL of PAA gave a polymer/DNA ratio of 25) were mixed and incubated at room temperature for 30 min. EB 5 μL (4 μg/mL) was then added, and the mixture was incubated for another 30 min. Fluorescence intensity at a wavelength of 608 nm was measured by SpectraMax M2e at an excitation wavelength of 510 nm.

Cytotoxicity Assay

OVCAR-3 cells were maintained in RPMI-1640 containing 10% FBS, streptomycin and penicillin at 37°C with 5% CO_2 humidified atmosphere. Cells were cultured in 96-well plates at an initial seeding density of 5,000 cells/well and grown for 24 h before treatment. LPEI 25k or PAA was added to the medium at polymer concentrations ranging from 0.0125 to 1 mg/mL followed by a 4-h incubation. The treated cells were then cultured in fresh medium for another 44 h. MTT reagent (10 μL) was added to each well and incubated for 5 h. Detergent reagent (100 μL) was added into each well and the plates were placed in incubator until all the crystals were dissolved. The absorbance at 570 nm in each well was recorded using a Model 680 microplate reader (Bio-Rad, Hercules, CA).

In Vitro Transfection Efficiency

OVCAR-3 cells were seeded into 96-well plates at a density of 20,000/well in 200 μL complete medium 24 h prior to transfection. The medium was removed and rinsed with PBS once. Polyplex solutions (100 μL) in FBS-free medium at a pDNA dose of 10 μg/mL were added to each well and cultured for 4 h. Then, the polyplex solutions were replaced with 200 μL complete medium. The cells were incubated for an additional 44 h. Cell culture lysis reagent (CCLR; Promega, 40 μL) was added into each well to lyse the cells. Each cell-lysis solution (40 μL) was mixed with 100 μL of luciferase assay reagent (Promega) and the luminance was measured by SpectraMax M2e at 570 nm.

Transfection Mechanisms Study

Chlopromazine (inhibitor of clathrin-mediated endocytosis, 10 μg/mL), Filipin III (inhibitor of caveolae-mediated endocytosis, 5 μg/mL), wortmannin (inhibitor of PI3K-mediated macropinocytosis, 2 μg/mL), or Filipin III (5 μg/mL) + wortmannin (2 μg/mL) was pre-incubated with the cells for 30 min before transfection in FBS-free medium. Then the medium was replaced by polyplex solutions at a pDNA dose of 10 μg/mL following the steps described in transfection efficiency.

Intracellular Localization by Confocal Laser Scanning Fluorescence Microscopy and Flow Cytometry

pDNA was labeled with Cy-5 (Mirus Bio) according to the manufacturer's instructions. Briefly, pDNA was mixed with Cy-5 *label*IT reagent and incubated at 37°C for 1 h. Sodium chloride and ethanol were applied to purify the pDNA after labeling. The solution was centrifuged, the pDNA pellet was dissolved in TE buffer, and the concentration of pDNA was measured at 260 nm by Nanodrop (ND-1000). Cell nuclei were stained with acridine orange (Sigma–Aldrich, St. Louis, MO).

OVCAR-3 cells were plated into glass-bottom petri dishes (MatTek, Ashland, MA) at 200,000 cells per dish in 2 mL complete medium and incubated for 24 h before use. The medium was replaced with polyplex solutions at the pDNA dose of 10 μg/mL and then cultured for 3 or 6 h. The cells were then rinsed with PBS twice before observation by confocal microscope (Zeiss 710, Oberkochen, Germany). Cy-5 was excited at 643 nm and its fluorescence emission was observed using a 670–710 nm band-pass filter. Acridine orange was excited at 488 nm and the emission was detected ranging from 560 to 600 nm. Transmission images were obtained in the same scan.

OVCAR-3 cells treated with transfection reagents were rinsed with PBS, detached by Trypsin and resuspended in PBS. Five thousand cells were then analyzed using flow cytometry (easyCyte 8HT; Millipore, Billerica, MA) and data analysis was performed by guavaSoft software (Millipore).

Results and Discussion

Synthesis and Characterization of Cationic Poly(amido amine)s

The reactivities of primary and secondary amine towards acrylamide depend on the solvent. In water, secondary amine reacts much faster with acrylamide than primary amine (Toueg and Prunet, 2007), but the reactivity reverses in DMF (Mather et al., 2006). The reaction of CBA and AEPZ in a mixed solvent produced PAAs with tunable degrees of branching by adjusting the DMF/H_2O ratio. In this study, the reaction conditions were controlled to produce PAAs with the same repeating units and molecular weights but different branched structures (Fig. 1).

The DBs of the PAAs were calculated according to the following equation, $DB = (D + T)/(D + T + L)$ (Hawker et al., 1991), where D, T, and L represented the fractions of the branched, terminal, and linear units, respectively. In DMF, the reaction produced linear PAA. In DMF/H_2O mixture (volume ratio of 4/1), the produced PAA

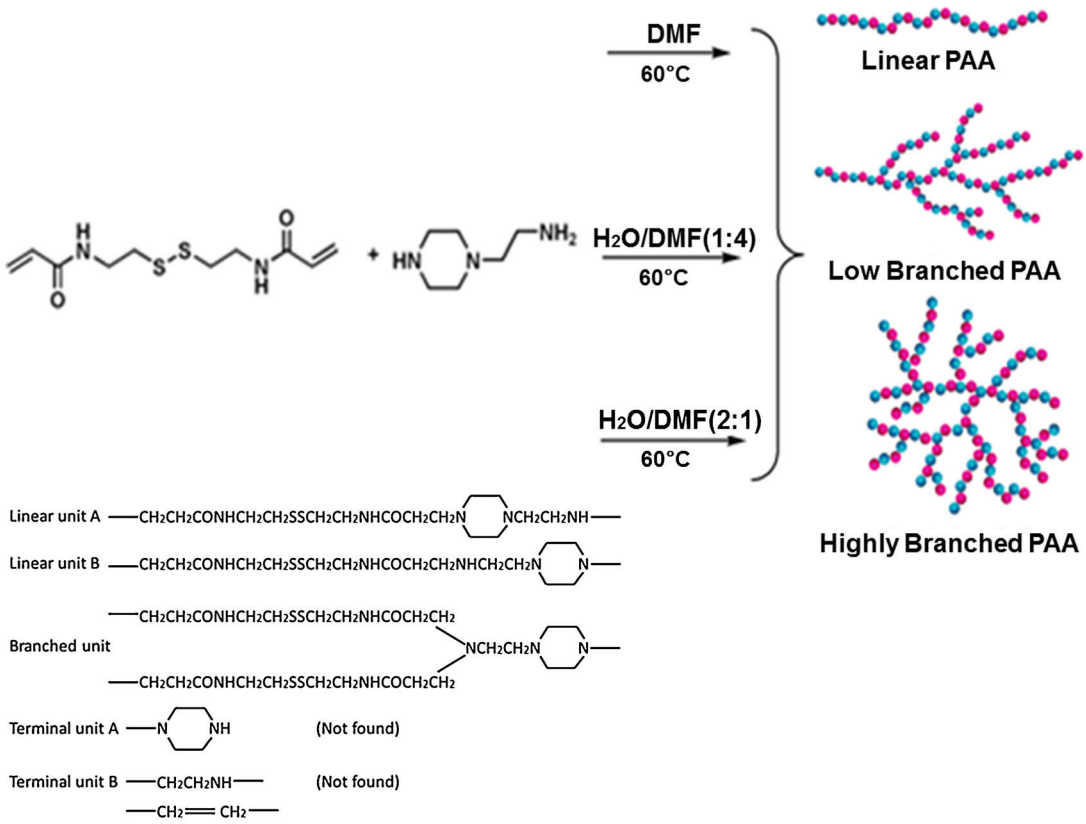

Figure 1. Synthesis route and schematic illustration of the molecular structure of PAAs.

was slightly branched. A highly branched PAA was obtained by carrying out the reaction in the presence of more H_2O (DMF/H_2O volume ratio of 1/2). The molecular weights of PAAs determined by MALDI-TOF (Table I) were about 4 KDa. These PAAs had approximately the same molecular weights but different pDNA binding capacities, cellular uptakes and transfection efficiencies, which were only attributed to their topological architectures.

Characterization of PAA Polyplexes

The complexation of PAA with pDNA was first probed by gel electrophoresis. As shown in Figure 2A, The PAAs with different DBs showed very different pDNA condensation ability. LPAA could completely retard pDNA migration at a polymer/DNA ratio of 25. LBPAA only partially retained pDNA at a polymer/DNA ratio of 1 but completely retained pDNA at a polymer/DNA ratio of 12.5. HBPAA had the strongest DNA condensation ability, completely retaining pDNA at a polymer/DNA ratio of 1. These polyplexes could be disrupted by cleaving the PAA disulfide linkages. After incubation with disulfide reducing agent DTT (10 mM) at 37°C for 1 h, free pDNA was released from the polyplexes, confirming the efficient intracellular release of pDNA from these bioreducible PAA polyplexes.

Table I. Reaction conditions and characterization data.

	DMF/H_2O	DB	Mn	PDI
LPAA	100/0	0	4,758	1.82
LBPAA	80/20	0.10	4,154	1.65
HBPAA	33/66	0.42	4,358	1.59

The sizes of the PAA polyplexes were measured using dynamic light scattering. Interestingly, only LBPAA effectively condensed pDNA into 130 nm nanoparticles—which was assumed necessary for efficient cellular uptake (Kazuo, 2011)—starting at a polymer/DNA ratio of 12.5 (Fig. 2B). In the case of HBPAA, the hydrodynamic diameter of the polyplexes was about 700 nm between polymer/DNA ratios of 12.5 and 100. The size of the LPAA polyplexes first increased with increasing polymer/DNA weight ratios (1–25), and then went down to 400 nm after increasing the polymer/DNA ratio to 100. This initial increase in the size of LPAA polyplexes could be attributed to the interactions among neutrally net charged nanoparticles at

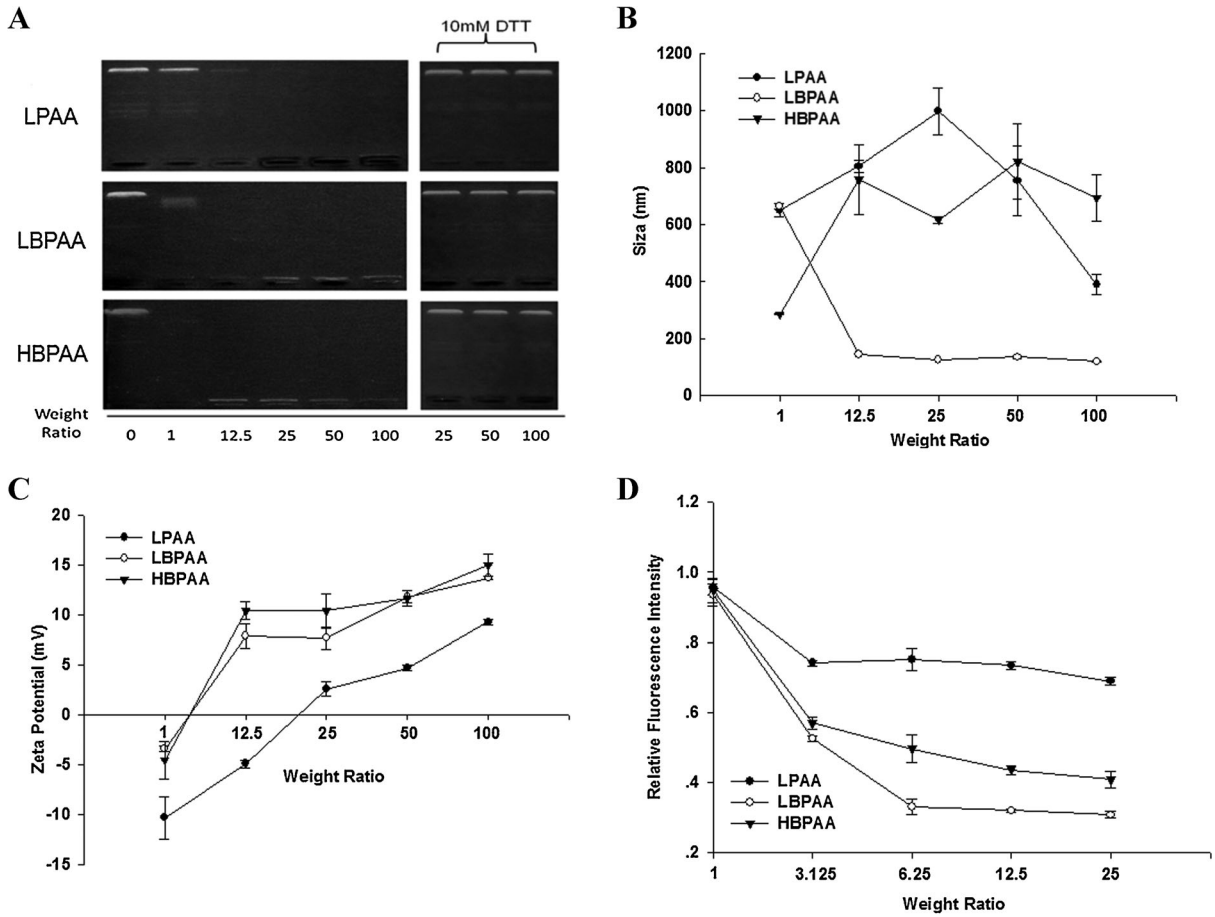

Figure 2. Agarose gel electrophoresis of PAA polyplexes with and without the presence of DTT as a function of polymer/DNA weight ratios (**A**). The left lane contained pDNA alone (no polymer) and was used as a control. Gel was run on 0.9% agarose gel at 100 mV for 40 min before UV observation. Average size (**B**) and zeta-potential (**C**) measurements of PAA polyplexes as a function of polymer/DNA ratios. Relative fluorescence units of EB exclusion assay (**D**): EB 5 μL (4 μg/mL) was added into the mixture of pDNA 50 μL (40 μg/mL) and equal volume of PAAs, and the mixture was incubated for 30 min. Then the emitted fluorescence was measured at an emission wavelength of 608 nm and an excitation wavelength of 510 nm.

low polymer/DNA ratios (Kim et al., 2004). The zeta-potential values of the polyplexes from LPAA were generally 7 mV lower than those from LBPAA or HBPAA at the same polymer/DNA ratios (Fig. 2C). The polyplexes of LBPAA and HBPAA started to be positively charged at a polymer/DNA ratio around 5, but for LPAA the ratio was higher than 20. The higher positive charge of branched PAA polyplexes, compared to their linear counterparts, is beneficial for efficient cell–membrane adhesion (Cho et al., 2009).

We quantitated the pDNA binding ability of PAAs using an EB replacement assay. EB competes with PAA to bind pDNA to form fluorescent EB/pDNA complexes. Adding EB to the PAA/pDNA polyplexes dissociates the polyplexes and increases the corresponding fluorescence. Thus, a lower fluorescence suggests a stronger PAA/pDNA binding affinity. The relative fluorescence units of EB/pDNA (no polymers) were set to 1. We found that the three PAAs showed very different pDNA binding ability. The presence of LBPAA substantially reduced the EB/pDNA fluorescence intensity and exhibited the strongest binding ability with pDNA (Fig. 2D). HBPAA had a slightly weaker DNA-binding capability than LBPAA, and the LPAA was the weakest. This is in agreement with the gel electrophoresis results that LPAA retained DNA only at the PAA/DNA ratio of 25 or higher.

Branched polymers were found to better condense pDNA than their linear counterparts, for example, branched PEI could form more stable nanoparticles than linear PEI, especially with siRNA (Kwok and Hart, 2011), probably because branched PEI tended to stay in the DNA major groove and interacted with both strands of the DNA (Sun et al., 2011). These findings show that branched cationic polymers generally had a higher DNA binding affinity than their linear counterparts. However, how the degree of branching would affect pDNA packaging was still an

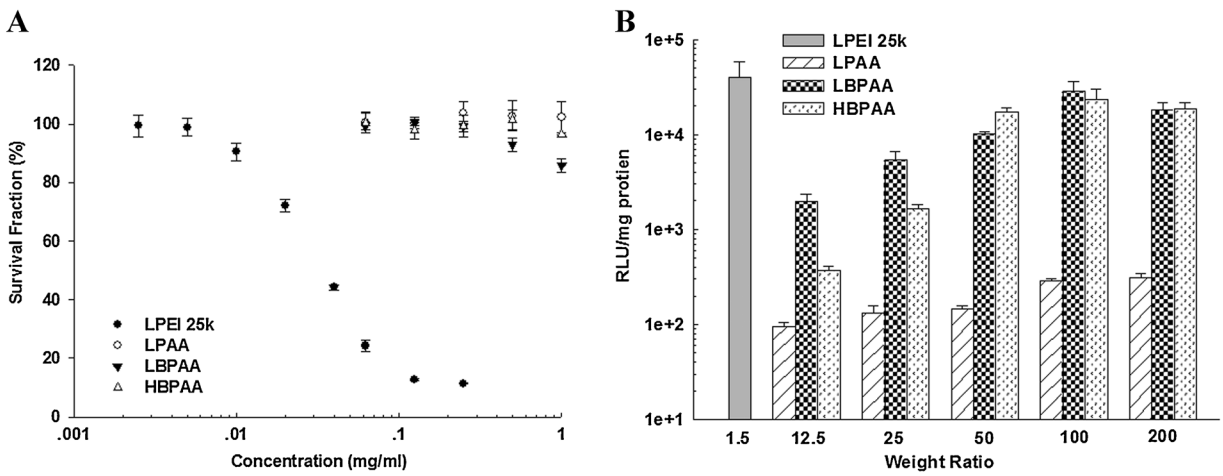

Figure 3. The cytotoxicity of PAAs and LPEI 25k on OVCAR-3 cells at various polymer concentrations (**A**). Cells were treated with polymers for 4 h and cultured in fresh medium for another 44 h before MTT assay. The transfection efficiencies of PAAs and LPEI 25k on OVCAR-3 cells (**B**). Cells were treated with polyplexes at different polymer/DNA ratios (pDNA dose of 10 μg/mL) for 4 h. The polyplex solution was then replaced with fresh medium and cultured for another 44 h before luciferase measurements.

enigma. Molecular dynamics simulation showed that intermediate graft lengths of polylysine exhibited a smaller binding free energy than the largest, the smallest graft or linear polylysine, and therefore had a higher transfection efficiency (Elder et al., 2011). Thus, in this study, the lower binding free energy endowed LBPAA with a better pDNA binding capacity than both HBPAA and LPAA.

Cytotoxicity

The in vitro cytotoxicity of PAAs to OVCAR-3 cells was evaluated as a function of polymer concentration (Fig. 3A). PAAs showed no or negligible cytotoxicity (survival rate $\geq$80%) at concentrations up to 1 mg/mL, while LPEI 25k already induced 90% cell death at 0.25 mg/mL, suggesting

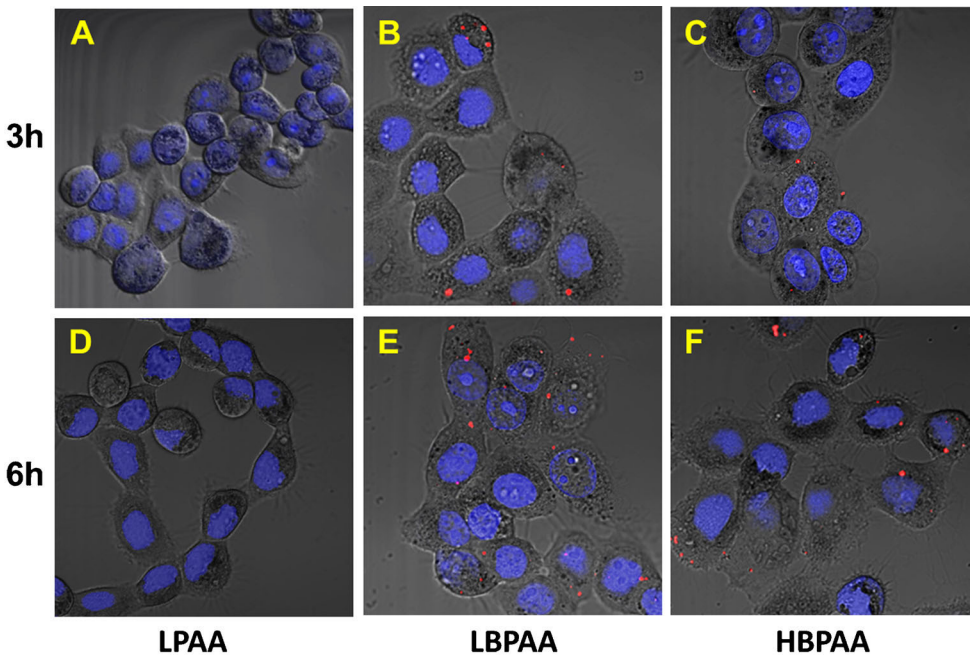

Figure 4. OVCAR-3 cells were treated with LPAA (**A**), LBPAA (**B**), and HBPAA (**C**) polyplexes for 3 h and LPAA (**D**), LBPAA (**E**), and HBPAA (**F**) polyplexes for 6 h before observation by confocal laser scanning microscopy. Cell nuclei were stained with acridine orange (blue) and pDNA was labeled with Cy5 (red). All these polyplexes had a polymer/DNA ratio of 25 at a pDNA dose of 10 μg/mL.

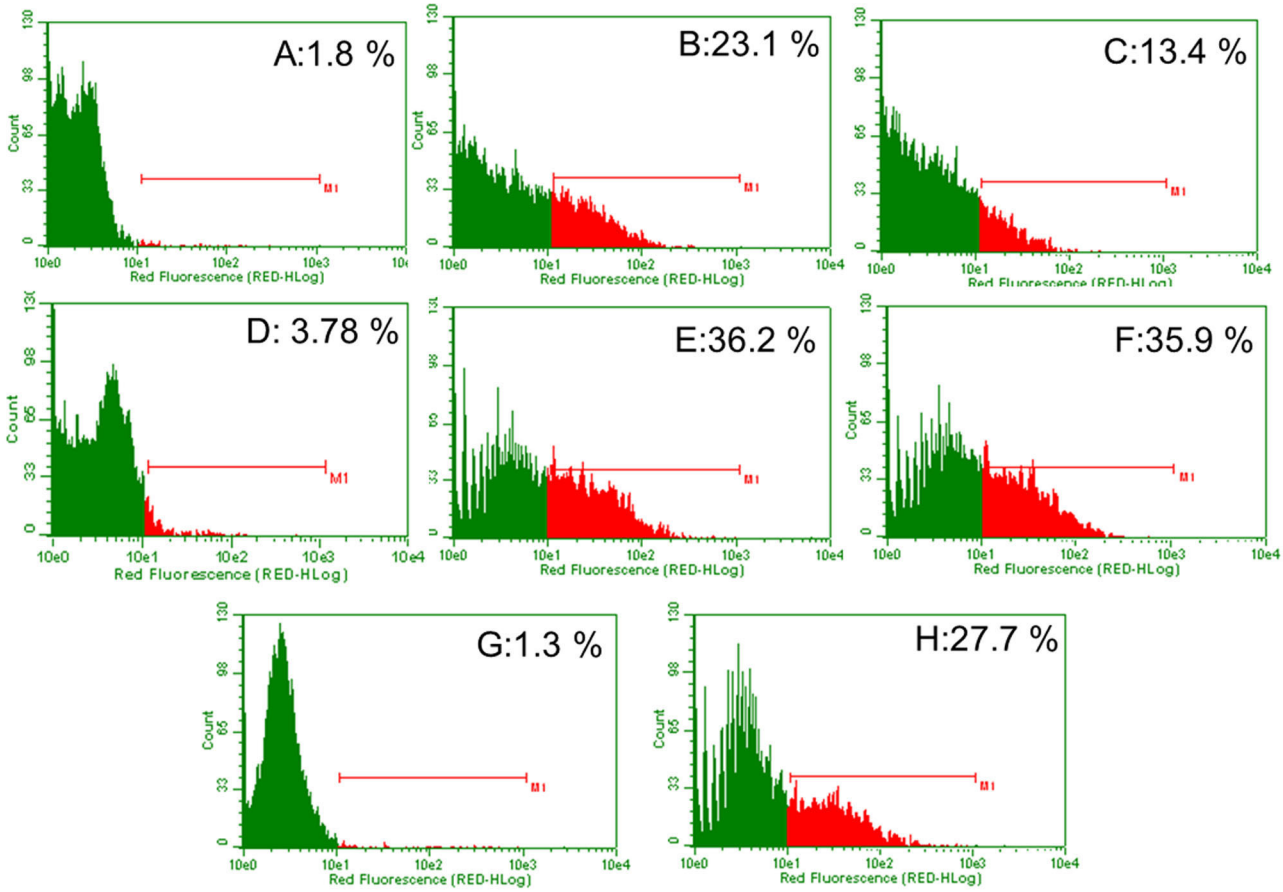

Figure 5. Quantification of cellular uptake by flow cytometry. OVCAR-3 cells only (no polymers and pDNA) were used as control (**G**). Polyplexes of LPAA (**A**), LBPAA (**B**), and HBPAA (**C**) at a polymer/DNA ratio of 25; polyplexes of LPAA (**D**), LBPAA (**E**), and HBPAA (**F**) at a polymer/DNA ratio of 100; and LPEI 25k polyplexes (**H**) at a polymer/DNA ratio of 1.5 were incubated with OVCAR-3 cells for 4 h before flow cytometric analysis. The pDNA dose was 10 μg/mL.

that the PAAs were much less toxic than LPEI 25k to OVCAR-3 cells. Although other reports demonstrated that at a given molecular weight, cytotoxicity of poly(2-(dimethylamino)ethyl methacrylate) (PDMAEMA) decreased with increasing the number of arms (Synatschke et al., 2011), here the topological effect on cytotoxicity was not seen in PAAs, probably due to the low molecular weight and their degradable property.

In Vitro Gene Transfection

Gene transfection efficiencies of PAAs and LPEI 25k polyplexes were measured in OVCAR-3 cells as a function of polymer/pDNA ratios (Fig. 3B). The transfection efficiency of LPAA polyplexes was much lower than both LBPAA and HBPAA polyplexes, especially at high polymer/DNA ratios. LBPAA polyplexes always had the highest transfection efficiency among the three polyplexes and the efficiency reached a maximum at a ratio of 100. The transfection efficiency of HBPAA polyplexes was relatively low at low polymer/DNA ratios (e.g., 25), but dramatically increased to a level comparable to LBPAA polyplexes at polymer/DNA ratios of 50 or higher. The highest transfection efficiency of PAA polyplexes was achieved by LBPAA polyplexes at a polymer/DNA ratio of 100, at which the transfection efficiency was comparable to that of LPEI 25k. Therefore LBPAA polyplexes could very efficiently transfect OVCAR-3 cells, and meanwhile caused negligible toxicity at the doses of transfection.

Cellular Uptake and Its Mechanisms

The topological effects of the different PAAs on their endocytosis pathways were probed using confocal microscopy and flow cytometry. OVCAR-3 cells were incubated with PAA polyplexes at a polymer/DNA ratio of 25 for either 3 or 6 h. Red signals indicated Cy-5-pDNA, and blue fluorescence marked the cell nucleus. As shown in Figure 4A and D, Cy-5-pDNA could not be seen in the cells treated with LPAA polyplexes at 3 or 6 h incubation.

After 3 h of incubation, more red signals were observed in the cells treated with LBPAA polyplexes (Fig. 4B) than those treated with HBPAA polyplexes (Fig. 4C) at a polymer/DNA ratio of 25. At 6 h incubation, punctuated red spots were found in most of the cells treated with LBPAA polyplexes, obviously more than that treated with HBPAA polyplexes (Fig. 4E and F).

Flow cytometry was then used to quantify the proportion of cells endocytosized with PAA/Cy-5-pDNA polyplexes. OVCAR-3 cells were treated with the polyplexes for 4 h before flow cytometric analysis. Again, almost no cells took up LPAA polyplexes at polymer/DNA ratios of 25 and 100 (Fig. 5A and D, respectively). At a polymer/DNA ratio of 25, twice as many cells were taking up LBPAA polyplexes compared to the HBPAA polyplexes. However, there was no difference in cellular uptake between LBPAA and HBPAA polyplexes at a polymer/DNA ratio of 100. Interestingly, more OVCAR-3 cells endocytosized LBPAA and HBPAA polyplexes (at a polymer/DNA ratio of 100) than LPEI 25k. These results suggested that LBPAA polyplexes could more efficiently enter into OVCAR-3 cells than HBPAA at a low polymer/DNA ratio, leading to higher transfection efficiency of LBPAA polyplexes than HBPAA polyplexes. But the cellular entry of the polyplexes became similar at high polymer/DNA ratios. This trend is consistent with the gene transfection results.

The endocytosis pathways of the PAA polyplexes were selectively inhibited using appropriate inhibitors. Chlorpromazine is an amphiphilic compound that prevents the recycling of clathrin proteins from endosomes back to the cell membranes and inhibits the formation of new clathrin-coated pits. Filipin III binds strongly to caveolae and inhibits endocytosis, and thereby prevents lipid raft-mediated endocytosis. Wortmannin inhibits macropinocytosis via the PI3K pathway (Vercauteren et al., 2011; Wipf and Halter, 2005; Yamano et al., 2011). Figure 6 shows the inhibitor effects on gene transfection. Pretreatment of cells with chlorpromazine did not affect the transfection efficiencies of both LBPAA and HBPAA. After pretreating the cells with Filipin III or wortmannin, the relative transfection efficiencies dramatically decreased, indicating inhibited endocytosis through caveolae and PI3K-mediated pathways (Fig. 6). A combinational use of Filipin III and wortmannin further decreased the transfection efficacy to $<20\%$ but not completely, suggesting the possible existence of other endocytosis pathways. This result indicated that the difference in gene transfection efficiencies of LBPAA and HBPAA polyplexes was not due to altered endocytosis pathways, but solely due to the endocytosis rate. Other reports also found that caveolae and PI3K-mediated pathways played important roles in the endocytosis of disulfide-based PAA polyplexes (Vercauteren et al., 2011). The superior aspect of the caveolae-mediated pathway is that the delivery cargoes may evade a degrading compartment by avoiding fusing into lysosomes (Pelkmans and Helenius, 2002).

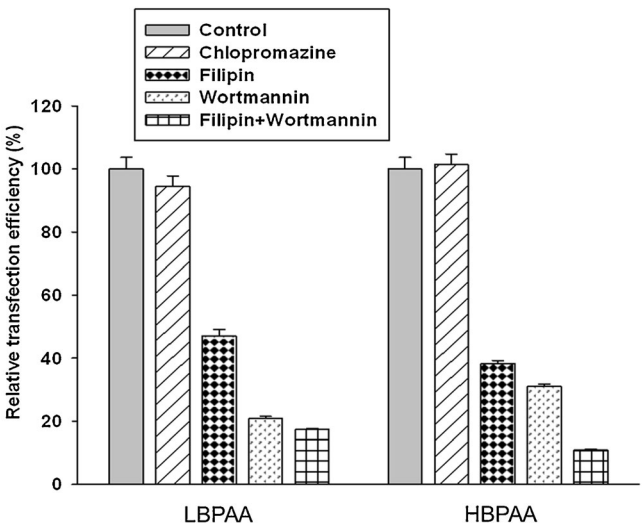

Figure 6. Endocytosis mechanisms of PAA polyplexes. The transfection efficiencies of LBPAA and HBPAA at a polymer/DNA ratio of 25 (pDNA dose 10 μg/mL) were used as a control. Cells were pretreated with chlorpromazine (10 μg/mL, inhibitor of clathrin-mediated pathway), Filipin III (5 μg/mL, inhibitor of caveolae-mediated pathway), wortmannin (2 μg/mL, inhibitor of macropinocytosis) alone, and Filipin III (5 μg/mL) + wortmannin (2 μg/mL), then LBPAA and HBPAA polyplexes were added into each well, followed by transfection efficiency measurements.

Conclusion

Branched PAAs were reported to better interweave with DNA than LPAA (Schallon et al., 2010), but branching of stiff structures would deteriorate its DNA condensation ability and transfection (Alhoranta et al., 2011). In this study, we synthesized three poly(amido amine)s to study the effects of topographical structures on pDNA binding, cellular uptake and gene transfection efficiency and found that the branching structure of PAA influenced its pDNA binding ability, cellular uptake and thereby the gene transfection efficiency. Low-branched PAA showed better pDNA binding, cellular uptake, and transfection than linear or highly branched ones. Therefore, this work provides another strategy to tune polymers as nonviral gene carriers.

References

Alhoranta AM, Lehtinen JK, Urtti AO, Butcher SJ, Aseyev VO, Tenhu HJ. 2011. Cationic amphiphilic star and linear block copolymers: Synthesis, self-Assembly, and in vitro gene transfection. Biomacromolecules 12(9):3213–3222.

Brumbach JH, Lin C, Yockman J, Kim WJ, Blevins KS, Engbersen JFJ, Feijen J, Kim SW. 2010. Mixtures of poly(triethylenetetramine/cystamine bisacrylamide) and poly(triethylenetetramine/cystamine bisacrylamide)-g-poly(ethylene glycol) for improved gene delivery. Bioconjug Chem 21(10):1753–1761.

Cho SK, Kwon YJ. 2012. Simultaneous gene transduction and silencing using stimuli-responsive viral/nonviral chimeric nanoparticles. Biomaterials 33(11):3316–3323.

Cho EC, Xie J, Wurm PA, Xia Y. 2009. Understanding the role of surface charges in cellular adsorption versus internalization by selectively removing gold nanoparticles on the cell surface with a I2/KI etchant. Nano Lett 9(3):1080–1084.

Dai Z, Gjetting T, Mattebjerg MA, Wu C, Andresen TL. 2011. Elucidating the interplay between DNA-condensing and free polycations in gene transfection through a mechanistic study of linear and branched PEI. Biomaterials 32(33):8626–8634.

Elder RM, Emrick T, Jayaraman A. 2011. Understanding the effect of polylysine architecture on DNA binding using molecular dynamics simulations. Biomacromolecules 12(11):3870–3879.

Emilitri E, Ranucci E, Ferruti P. 2005. New poly(amidoamine)s containing disulfide linkages in their main chain. J Polym Sci Pol Chem 43(7): 1404–1416.

Han L, Huang R, Li J, Liu S, Huang S, Jiang C. 2011. Plasmid pORF-hTRAIL and doxorubicin co-delivery targeting to tumor using peptide-conjugated polyamidoamine dendrimer. Biomaterials 32(4):1242–1252.

Hawker CJ, Lee R, Frechet JMJ. 1991. One-step synthesis of hyperbranched dendritic polyesters. J Am Cheml Soc 113(12):4583–4588.

Jiang X, Liu J, Xu L, Zhuo R. 2011. Disulfide-containing hyperbranched polyethylenimine derivatives via click chemistry for nonviral gene delivery. Macromol Chem Phys 212(1):64–71.

Kazuo M. 2011. Intracellular targeting delivery of liposomal drugs to solid tumors based on EPR effects. Adv Drug Deliver Rev 63(3):161–169.

Kibria G, Hatakeyama H, Ohga N, Hida K, Harashima H. 2011. Dual-ligand modification of PEGylated liposomes shows better cell selectivity and efficient gene delivery. J Control Release 153(2):141–148.

Kim TI, Seo HJ, Choi JS, Jang HS, Baek JU, Kim K, Park JS. 2004. PAMAM-PEG-PAMAM: Novel triblock copolymer as a biocompatible and efficient gene delivery carrier. Biomacromolecules 5(6):2487–2492.

Kwok A, Hart SL. 2011. Comparative structural and functional studies of nanoparticle formulations for DNA and siRNA delivery. Nanomedicine 7(2):210–219.

Lin C, Engbersen JFJ. 2008. Effect of chemical functionalities in poly(amido amine)s for non-viral gene transfection. J Control Release 132(3): 267–272.

Liu J, Jiang X, Xu L, Wang X, Hennink Wim E, Zhuo R. 2010. Novel reduction-responsive cross-linked polyethylenimine derivatives by click chemistry for nonviral gene delivery. Bioconjug Chem 21(10): 1827–1835.

Mather BD, Viswanathan K, Miller KM, Long TE. 2006. Michael addition reactions in macromolecular design for emerging technologies. Prog Polym Sci 31(5):487–531.

Meng F, Hennink WE, Zhong Z. 2009. Reduction-sensitive polymers and bioconjugates for biomedical applications. Biomaterials 30(12): 2180–2198.

Ou M, Wang XL, Xu R, Chang CW, Bull DA, Kim SW. 2008. Novel biodegradable poly(disulfide amine)s for gene delivery with high efficiency and low cytotoxicity. Bioconjugate Chem 19(3):626–633.

Ou M, Xu R, Kim Sun H, Bull David A, Kim Sung W. 2009. A family of bioreducible poly(disulfide amine)s for gene delivery. Biomaterials 30(29):5804–5814.

Parhamifar L, Larsen AK, Hunter AC, Andresen TL, Moghimi SM. 2010. Polycation cytotoxicity: A delicate matter for nucleic acid therapy-focus on polyethylenimine. Soft Matter 6(17):4001–4009.

Pelkmans L, Helenius A. 2002. Endocytosis via caveolae. Traffic 3(5): 311–320.

Piest M, Engbersen JFJ. 2010. Effects of charge density and hydrophobicity: Acetylation versus benzoylation of amino butyl SS-PAAS for gene delivery. J Control Release 148(1):e92–e94.

Schallon A, Jérôme V, Walther A, Synatschke CV, Müller AHE, Freitag R. 2010. Performance of three PDMAEMA-based polycation architectures as gene delivery agents in comparison to linear and branched PEI. React Funct Polym 70(1):1–10.

Sun YX, Zeng X, Meng QF, Zhang XZ, Cheng SX, Zhuo RX. 2008. The influence of RGD addition on the gene transfer characteristics of disulfide-containing polyethyleneimine/DNA complexes. Biomaterials 29(32):4356–4365.

Sun C, Tang T, Uludağ H, Cuervo Javier E. 2011. Molecular dynamics simulations of DNA/PEI complexes: Effect of PEI branching and protonation state. Biophys J 100(11):2754–2763.

Synatschke CV, Schallon A, Jérôme V, Freitag R, Müller AHE. 2011. Influence of polymer architecture and molecular weight of poly(2-(dimethylamino)ethyl methacrylate) polycations on transfection efficiency and cell viability in gene delivery. Biomacromolecules 12(12): 4247–4255.

Tang MX, Redemann CT, Szoka FC. 1996. In vitro gene delivery by degraded polyamidoamine dendrimers. Bioconjug Chem 7(6): 703–714.

Thomas CE, Ehrhardt A, Kay MA. 2003. Progress and problems with the use of viral vectors for gene therapy. Nat Rev Genet 4(5):346–358.

Toueg J, Prunet J. 2007. Dramatic solvent effect on the diastereoselectivity of michael addition: Study toward the synthesis of the ABC ring system of hexacyclinic acid. Org Lett 10(1):45–48.

Tzeng SY, Guerrero-Cázares H, Martinez EE, Sunshine JC, Quiñones-Hinojosa A, Green JJ. 2011. Non-viral gene delivery nanoparticles based on Poly(β-amino esters) for treatment of glioblastoma. Biomaterials 32(23):5402–5410.

Vader P, van der Aa Leonardus J, Engbersen Johan FJ, Storm G, Schiffelers Raymond M. 2011. Disulfide-based poly(amido amine)s for siRNA delivery: Effects of structure on siRNA complexation, cellular uptake, gene silencing and toxicity. Pharm Res 28(5):1013–1022.

Vercauteren D, Piest M, van der Aa LJ, Al Soraj M, Jones AT, Engbersen JFJ, De Smedt SC, Braeckmans K. 2011. Flotillin-dependent endocytosis and a phagocytosis-like mechanism for cellular internalization of disulfide-based poly(amido amine)/DNA polyplexes. Biomaterials 32(11):3072–3084.

von Erlach T, Zwicker S, Pidhatika B, Konradi R, Textor M, Hall H, Lühmann T. 2011. Formation and characterization of DNA-polymer-condensates based on poly(2-methyl-2-oxazoline) grafted poly(l-lysine) for non-viral delivery of therapeutic DNA. Biomaterials 32(22):5291–5303.

Wang RB, Zhou LZ, Zhou YF, Li GL, Zhu XY, Gu HC, Jiang XL, Li HQ, Wu JL, He L, Guo XQ, Zhu BS, Yan DY. 2010. Synthesis and gene delivery of poly(amido amine)s with different branched architecture. Biomacromolecules 11(2):489–495.

Wipf P, Halter RJ. 2005. Chemistry and biology of wortmannin. Org Biomol Chem 3(11):2053–2061.

Wu D, Liu Y, He C, Chung T, Goh S. 2004. Effects of chemistries of trifunctional amines on mechanisms of michael addition polymerizations with diacrylates. Macromolecules 37(18):6763–6770.

Yamano S, Dai J, Yuvienco C, Khapli S, Moursi AM, Montclare JK. 2011. Modified Tat peptide with cationic lipids enhances gene transfection efficiency via temperature-dependent and caveolae-mediated endocytosis. J Control Release 152(2):278–285.

Yang W, Pan CY, Liu XQ, Wang J. 2011. Multiple functional hyperbranched poly(amido amine) nanoparticles: Synthesis and application in cell imaging. Biomacromolecules 12(5):1523–1531.

Zeng X, Sun YX, Qu W, Zhang XZ, Zhuo RX. 2010. Biotinylated transferrin/avidin/biotinylated disulfide containing PEI bioconjugates mediated p53 gene delivery system for tumor targeted transfection. Biomaterials 31(17):4771–4780.

Zhou Y, Huang W, Liu J, Zhu X, Yan D. 2010. Self-assembly of hyperbranched polymers and its biomedical applications. Adv Mater 22(41):4567–4590.

Zhu X, Zhou Y, Yan D. 2011. Influence of branching architecture on polymer properties. J Polym Sci Pol Phys 49(18):1277–1286.